EPJ Web of Conferences **37**, 01018 (2012)
DOI: 10.1051/epjconf/20123701018

Exclusive vector mesons at high energies: from photon-proton to proton-proton and nucleus-nucleus collisions

Wolfgang Schäfer[a]

Institute of Nuclear Physics PAN, Cracow, Poland

Abstract. Photoproduction of vector mesons has been studied since the 1960's and was instrumental in establishing the hadronic structure of the photon and the concept of vector-meson dominance. More recently our knowledge on vector meson photoproduction has been furthered by experiments at the HERA accelerator. Total cross sections ans well as a number of kinematical distributions have been measured from light to heavy vector mesons. These experiments have been a testbed of ideas on the production mechanism, the QCD Pomeron exchange. In particular in varying the mass of the vector meson we can study the Pomeron exchange from the soft to the perturbatively hard regimes. The production mechanism also contains information on the quark-antiquark wave function of the produced meson. High energy protons or ions are the source of a flux of Weizsäcker-Williams photons, which can be utilized to study the photoproduction of vector mesons also at the Tevatron and LHC colliders. We discuss how information on the small-x gluon distribution in protons in nuclei can be obtained. Besides this intrinsic interest in vector meson production, a precise knowledge thereof is also necessary for odderon searches. In this regard, we discuss also transverse momentum distributions including absorption effects.

1 Introduction

The earliest investigations of diffractive photoproduction established the hadronic structure of the photon and were mainly based on the concept of vector-meson dominance. (For a review of these early developments, see e.g. [1].) More recently, the subject has been much advanced by experiments at the HERA accelerator. A wealth of physics information has been obtained from data: from transverse momentum distributions to total cross sections, to studies of s-channel helicity violation from the spin density matrix of vector mesons. Also the previously unexplored region of large photon virtuality Q^2 was thoroughly investigated. We cannot do justice here to the impressive amount of data and the various approaches proposed and conclusions reached by theorists. Instead we refer to the recent review [2]. The exclusive photoproduction of vector mesons at high energies is a typical diffractive process, which in the Regge theory is described by the t-channel exchange of a Pomeron (see e.g. the recent textbooks [3]). Consequently, these experiments have been important for testing ideas on the production mechanism, the QCD Pomeron exchange. In particular in varying the mass of the vector meson we can study the Pomeron exchange from the soft to the perturbatively hard regimes. The production mechanism also contains information on the quark-antiquark wave function of the produced meson.

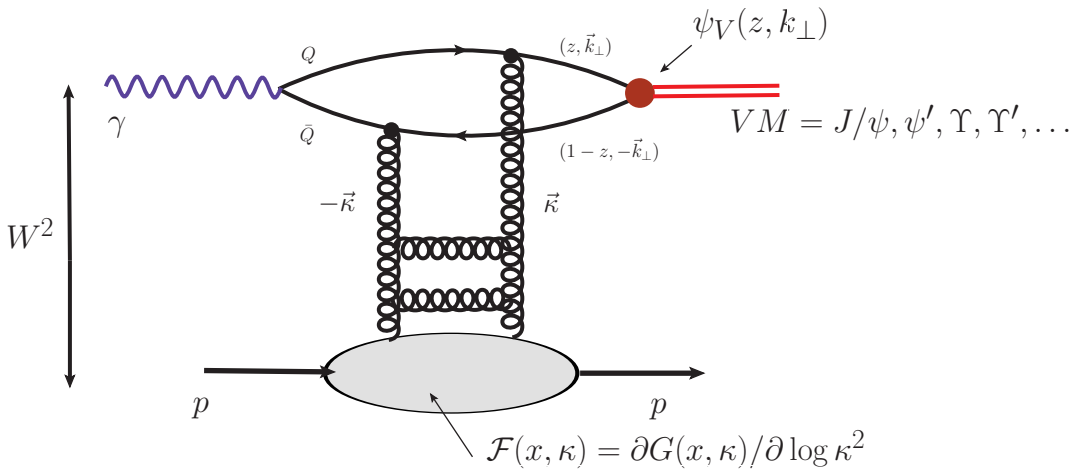

Fig. 1. A typical Feynman diagram for the $\gamma p \to Vp$ amplitude. The $\gamma \to Q\bar{Q}$ vertex is calculated perturbatively. Nonperturbative information is contained in the light cone wave function of the vector meson and the unintegrated gluon distribution.

2 Photoproduction $\gamma p \to Vp$ at high energies

One of the most striking findings of the diffractive vector meson studies at HERA concerns the systematics of the energy-dependence of the various total vector-meson cross sections. Indeed, if, motivated by Regge theory, we parametrize the dependence on γp center-of-mass energy W, as

$$\sigma_{\rm tot}(\gamma p \to Vp) \propto \left(\frac{W^2}{W_0^2}\right)^{\delta}, \tag{1}$$

the effective intercept δ turns out do be a function of the hard scale $Q^2_{\rm eff} = Q^2 + M_V^2$. Here Q^2 is the photon virtuality, M_V the mass of the vector meson. For the case photoproduction, of most interest in this presentation, one finds the following: firstly, for light vector mesons ρ^0, ω, and also for ϕ, we have $\delta \sim 0.11$, close to the "soft Pomeron" intercept of $\delta \sim 0.08$ that rules, e.g. the total photoabsorption cross section. The intercept then significantly increases with meson mass: for J/ψ, $\delta \sim 0.4$, for $\psi(2S)$, we have $\delta \sim 0.55$, and for Υ, the few available data points are consistent with $\delta \sim 0.6$. Given these process-dependent intercepts, do we have to give up the concept of a Pomeron? How can this behaviour be obtained in a "microscopic" approach? Indeed such a systematics of the energy dependence is qualitatively easily understood within the color-dipole approach [4,**?**] to hard and soft diffractive processes. Within the color-dipole framework, the hadronic structure of the photon is exhausted by QCD degrees of freedom, at lowest order quark-antiquark pairs. The forward diffractive amplitude shown in Fig. 1 takes the form

$$\Im m A(\gamma^*(Q^2)p \to Vp; W, t=0) = \int_0^1 dz \int d^2\boldsymbol{r}\, \psi_V(z,\boldsymbol{r})\, \psi_{\gamma^*}(z,\boldsymbol{r},Q^2)\, \sigma(x,\boldsymbol{r}), \tag{2}$$

where $x = M_V^2/W^2$, ψ_V and ψ_γ are the light-cone wave functions for the quark-antiquark Fock states of the vector meson and photon respectively. The $q\bar{q}$ separation $\boldsymbol{r}$ is conserved during the interaction (and so are the longitudinal momentum fractions $z, 1-z$ carried by q and $\bar{q}$). Color dipoles of size $\boldsymbol{r}$ are diagonal states of the S-matrix and interact with the proton with the cross section

$$\sigma(x,\boldsymbol{r}) = \frac{4\pi}{3}\alpha_S \int \frac{d^2\boldsymbol{\kappa}}{\boldsymbol{\kappa}^4} \frac{\partial x g(x,\boldsymbol{\kappa}^2)}{\partial \log(\boldsymbol{\kappa}^2)} \Big[1 - \exp(i\boldsymbol{\kappa}\boldsymbol{r})\Big], \tag{3}$$

[a] e-mail: Wolfgang.Schafer@ifj.edu.pl

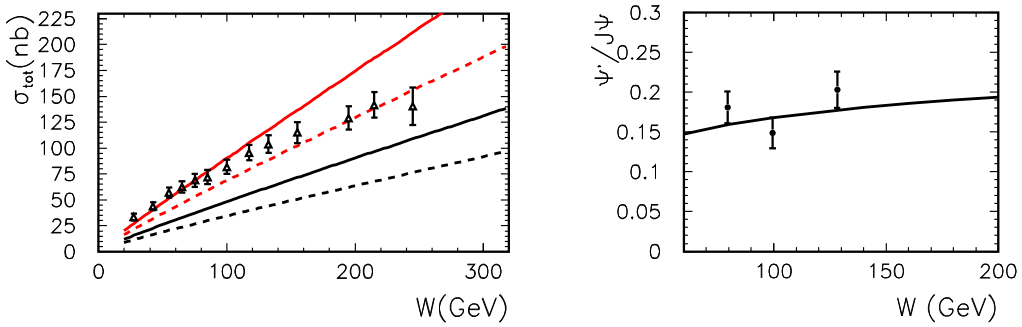

Fig. 2. Left panel: the total cross section for $\gamma p \to J/\psi p$. Data from the ZEUS collaboration. Red lines are for a Gaussian, the black ones for a Coulomb-type wave function. Solid lines include an NLO treatment of the vector meson decay width, while the dashed lines a LO one. Right panel: The ratio of total cross sections of $\psi(2S)$ and J/ψ photoproduction. Here a Gaussian wave function was used.

which in turn is related to the transverse-momentum dependent (or unintegrated) gluon distribution (see e.g. [5] and references therein). Let us try to understand the behaviour of the amplitude (2) at large $Q^2_{\rm eff}$: firstly, the photon's light cone wave function falls off as

$$\psi_{\gamma^*}(z, \mathbf{r}, Q^2) \propto \exp[-\varepsilon r]\,,\ \varepsilon = \sqrt{m_f^2 + z(1-z)Q^2}\,, \tag{4}$$

which together with the fact that the distribution of dipoles in the meson is a smooth nonsingular function leads to the fact that the overlap (2) is dominated by dipoles of size [4]

$$r \sim r_S \approx \frac{6}{\sqrt{Q^2 + M_V^2}}\,, \tag{5}$$

which has become known as the "scanning radius". For a quick estimate of the asymptotic behaviour, one can expand the exponential in eq.(3), so that for small dipoles:

$$\sigma(x, r) = \frac{\pi^2}{3} r^2 \alpha_S(q^2) x g(x, q^2)\,,\ q^2 \approx \frac{10}{r^2}\,, \tag{6}$$

which, when inserted into (2) in conjunction with (4,5) leads to [4]:

$$\Im m\, A(\gamma^* p \to V p) \propto r_S^2 \sigma(x, r_S) \propto \frac{1}{Q^2 + M_V^2} \times \frac{1}{Q^2 + M_V^2}\, x g(x, Q^2 + M_V^2)\,. \tag{7}$$

Notice the strong deviation from the $(Q^2 + M_V^2)^{-1}$ pole behaviour predicted by vector meson dominance. Hadronic degrees of freedom are not a good vantage point at all in this case. In fact, one of the factors $r_S^2 \propto (Q^2 + M_V^2)^{-1}$ comes from the shrinking with Q^2 and m_Q^2 overlap of the photon and meson dipole distributions, a second factor of r_S^2 originates from the interaction probability of a small dipole, which decreases $\propto r^2$ (color transparency). Finally, there is the important dependence on $Q^2 + M_V^2$ through the argument of the gluon distribution. It gives us the sought-for correlation between energy dependence and $Q^2 + M_V^2$. Indeed, empirically, from DGLAP fits we know that $x g(x, \mu^2) \propto (1/x)^{\lambda(\mu^2)}$ with $\lambda(\mu^2) \sim 0.1 \div 0.4$ for $\mu^2 = 1 \div 10^2\,{\rm GeV}^2$. In practical calculations, one would not use the approximation (6), but rather the full fledged (2,3). Its translation to momentum space can be found in [2] and was used in [6–9]. As default, we use an unintegrated gluon distribution adjusted to inclusive HERA data in [5]. In Fig. 2 we show results from [7] for J/ψ and its first excited state $\psi(2S)$. The suppression of $\psi(2S)$ production is a meson structure effect: the node in the $\psi(2S)$ wave function entails

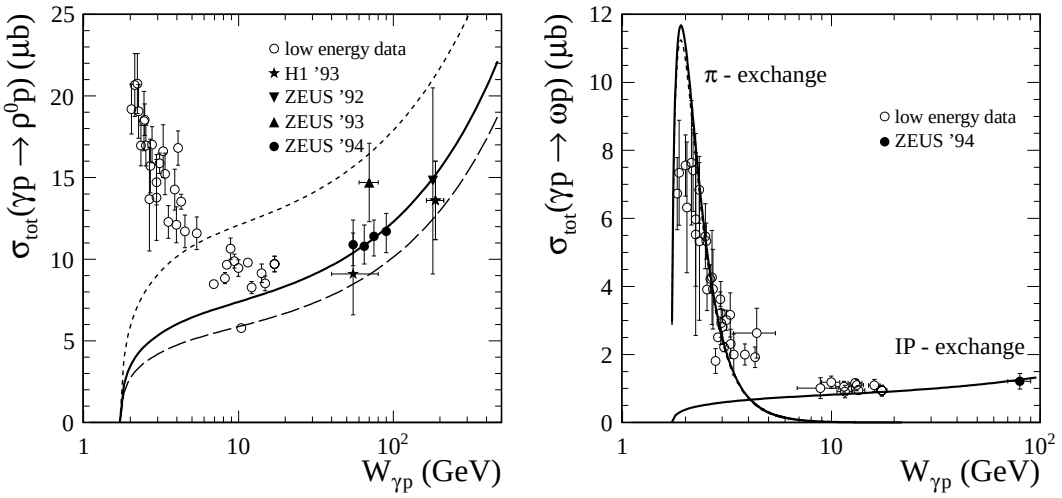

Fig. 3. Total cross sections for the production of light vector mesons. Left panel: ρ^0 production. The different curves show the variation with a change of the constituent quark mass [9]. Below $W \sim 10\,\mathrm{GeV}$ secondary Reggeons must be included. Right panel: ω production. Here the same quark mass that gives the best fit to ρ^0 production was used for the Pomeron exchange contribution. At low energies also the contribution from pion exchange via the anomalous $\gamma\pi\omega$-vertex is included.

cancellations in the production amplitude, as it was long ago found within the color dipole models [4]. Reasonable agreement with HERA data is also obtained for Υ production [6]. Notice, that for heavy vector mesons, the relevant dipole sizes are small (the scanning property!), and we are in the perturbative regime, where the gluon distribution is legitimately used. The dipole factorization (2) doesn't in fact rely on perturbation theory, it is the relation between dipole cross section and gluon distribution that does. Color dipoles are good degrees of freedom also in the nonperturbative regime: following [4], just allowing for a constituent mass of quarks in the loop allows for a satisfactory description also of ϕ [8], and even ρ^0, ω [9] production (see Fig. 3).

3 Central exclusive photoproduction in proton-(anti)proton collisions

Now, that we have convinced ourselves, that diffractive photoproduction of heavy vector mesons (especially its energy dependence) is a sensitive probe of the gluon distribution distribution, let us turn to proton-(anti)proton collisions, where in fact very high energy photoproduction is accessible today. Indeed, being charged particles, fast protons give rise to a flux of Weizsäcker-Williams photons. Clearly, in distinction to pointlike electrons, the finite-size protons will only supply us with quasi-real $Q^2 \sim 0$ photons, so that the perturbative regime is accessible only for heavy quarks/mesons. There is a second complication: either of the colliding protons can emit the photon, and the amplitudes for these two processes interfere. Additionally, we have to take into account, that protons may also interact strongly - the absorptive or unitarity correction. Those aspects are discussed in quite some detail in [10]. Here we show our results for the rapidity spectrum of exclusive vector mesons at Tevatron and LHC energies. At Tevatron energies, at central rapidities the subprocess energies for $\gamma p \to Vp$ or $\gamma \bar{p} \to V\bar{p}$ cover the known HERA domain. Given the fact that absorptive corrections, due to the peripheral nature of the reaction are weak, this means that robust predictions of vector meson production are possible. At LHC energies, it is possible to extend the energy range over the one already studied at HERA. For example, for J/ψ production at central rapidity $y = 0$, we have $W_{\gamma p} \sim 140\,\mathrm{GeV}$, whereas at $y = 4$ the photoproduction amplitude at $W_{\gamma p} \sim 1\,\mathrm{TeV}$ enters. Results of our calculations are shown in Figs. 4, 5. Also shown there, for J/ψ production is a data point obtained by the CDF collaboration at the Tevatron [11]. As we see it is well described by our calculation, no additional contribution as for example an

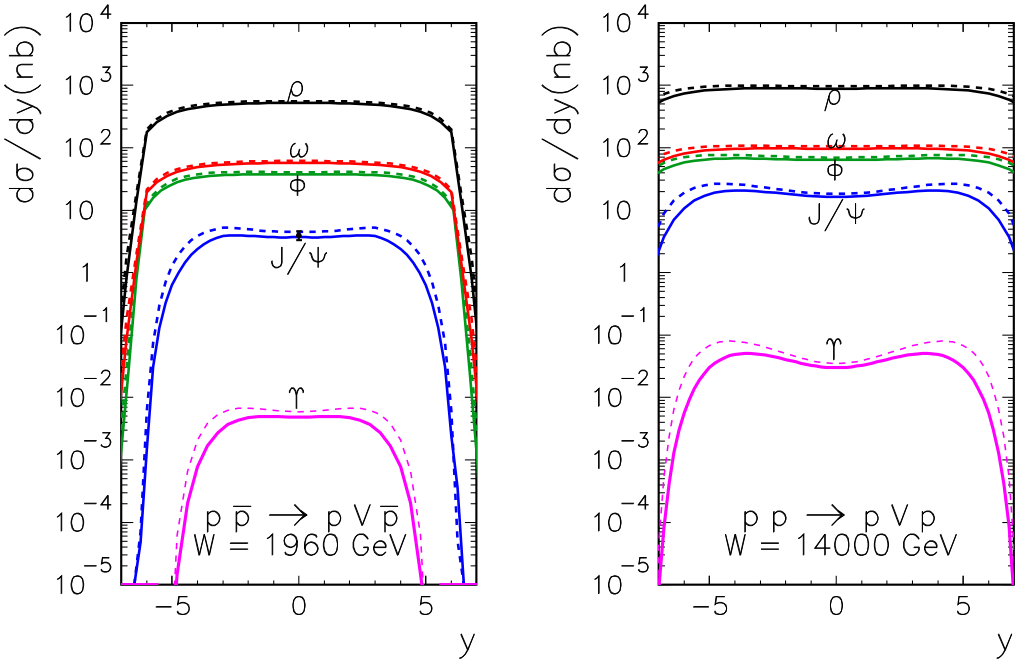

Fig. 4. Rapidity dependence of central exclusive vector meson production in proton-(anti)proton collisions. Left panel: proton-antiproton collisions at W=1960 GeV. Right panel: proton-proton collisions at W=14 TeV. In the left panel also shown is the data point from the CDF collaboration. Dashed lines are without absorptive corrections, while solid lines include them.

Odderon is required. In Fig. 5 we show results for two different unintegrated gluon distributions in a proton: the curves labeled IN use the glue from [5], whereas the ones labeled KS the one from [12]. The latter is obtained from a nonlinear evolution equation which accounts for the physics of gluon saturation at small x, while the former does not include explicit saturation effects. We observe that the shape of rapidity spectra is strongly affected, as well as the size of the cross section predicted at LHC energies.

An interesting pattern was found in our calculations [9] of exclusive ω production, see Fig. 5. Here we deal with a purely soft process where there is no controlled access to the unintegrated gluon distribution. Here, in addition to photoproduction we also included a number of purely strong interaction processes. The ωNN coupling is large, and there are "bremsstrahlung" type of contributions, where the ω is emitted off a nucleon line and which dominate in the respective beam and target fragmentation regions. They are the typical example of diffractive dissociation of a proton into a low-mass continuum state. In addition, there are contributions, which contain the ω Reggeon exchange in the crossed channel (the ω-Pomeron fusion). Although the ω trajectory is subleading, they can be numerically surprisingly large.

4 From the free nucleon to the nuclear target: γA and AA collisions

We now turn to another type of reactions, where the exclusive vector meson production can reveal precious information: nucleus-nucleus collisions. Collisions of heavy ions are the classic domain "Weizsäcker-Williams"(WW)-physics [13], clearly because of the large electromagnetic charges involved. Here we present our calculations from Ref. [14]. We constructed the unintegrated gluon distribution of the nucleus at $x \sim 0.01$ following [15], where as an input only the gluon distribution of the free nucleon is needed. Such a gluon distribution contains multiple scattering effects and sums up

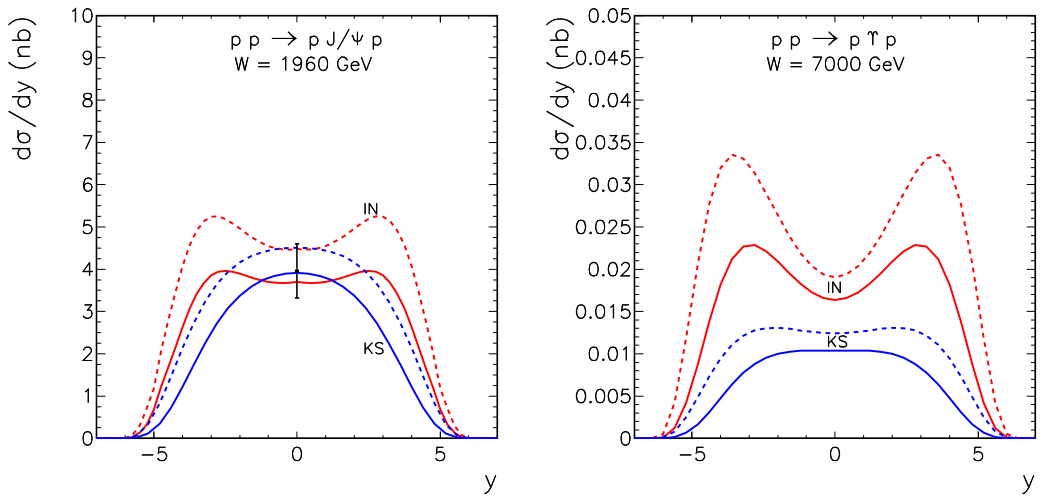

Fig. 5. Rapidity dependence of central exclusive vector meson production in proton-(anti)proton collisions for different unintegrated gluon distributions in a proton (see text). Dashed lines do not include absorptive corrections, while solid ones do. Left panel: J/ψ production at the Tevatron energy W=1960 GeV. Right panel: Υ production at an LHC energy, W=7 TeV. In the left panel also shown is the data point from the CDF collaboration.

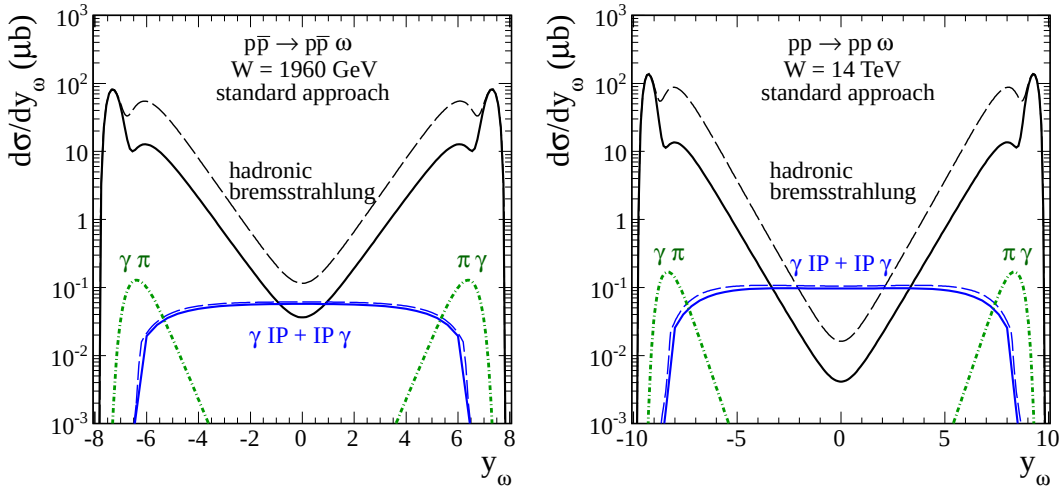

Fig. 6. Rapidity dependence of exclusive ω meson production in proton-(anti)proton collisions. Left panel: $p\bar{p}$ collisions at W=1960 GeV. Right panel: pp collisions at W=7 TeV. Shown are the contributions from hadronic "bremsstrahlung", from photoproduction (γ-Pomeron fusion) as well as a contribution from the anomalous $\gamma\pi\omega$ vertex. From [9].

Feynman diagrams as the ones shown in Fig. 7. To include the effects of nonlinear small-x evolution, we include the $q\bar{q}g$–Fock state and its rescatterings. Here we follow [16] where such a procedure has been successfully pursued for nuclear structure functions. Our predictions for LHC energies, which can be checked by the ALICE collaboration are shown in Fig. 8. Here the coherent vector meson production gives us a rare access to the small-x glue in a nucleus.

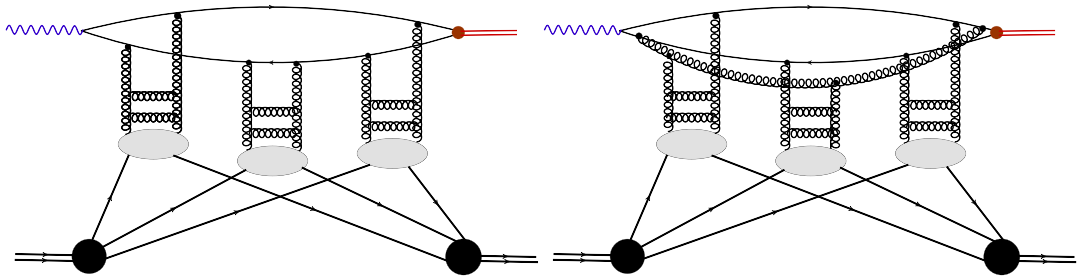

Fig. 7. Two Feynman diagrams for the $\gamma p \to Vp$ amplitude on the nuclear target. The left diagram represents a rescattering of the $Q\bar{Q}$-Fock state and dominates at not too small values of x. The diagram on the right hand side can be viewed as a rescattering of a $Q\bar{Q}g$-Fock state. It is responsible for the x-dependence of the amplitude at small x.

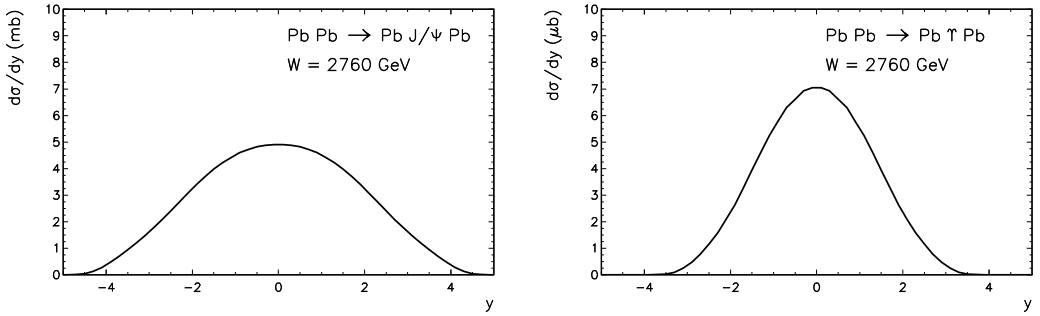

Fig. 8. Rapidity dependence of exclusive J/ψ-production (left) and Υ production (right) in lead-lead collisions at the LHC energy $W_{NN} = 2.76$ TeV [14].

References

1. T. H. Bauer, R. D. Spital, D. R. Yennie and F. M. Pipkin, Rev. Mod. Phys. **50** (1978) 261 [Erratum-ibid. **51** (1979) 407].
2. I. P. Ivanov, N. N. Nikolaev and A. A. Savin, Phys. Part. Nucl. **37** (2006) 1.
3. V. Barone and E. Predazzi, *High-energy particle diffraction* (Springer, Berlin 2002); S. Donnachie, H. G. Dosch, O. Nachtmann and P. Landshoff, Camb. Monogr. Part. Phys. Nucl. Phys. Cosmol. **19** (2002) 1.
4. N. N. Nikolaev, Comments Nucl. Part. Phys. **21** (1992) 41; J. Nemchik, N. N. Nikolaev, E. Predazzi and B. G. Zakharov, Z. Phys. C **75** (1997) 71 .
5. I. P. Ivanov and N. N. Nikolaev, Phys. Rev. D **65** (2002) 054004 [hep-ph/0004206].
6. A. Rybarska, W. Schäfer and A. Szczurek, Phys. Lett. B **668** (2008) 126.
7. A. Cisek, *Exclusive processes with large rapidity gaps in the formalism of unintegrated gluon distributions*, (PhD thesis, The Henryk Niewodniczański Institute of Nuclear Physics, Polish Academy of Sciences, Kraków, 2012)
8. A. Cisek, W. Schäfer and A. Szczurek, Phys. Lett. B **690** (2010) 168.
9. A. Cisek, P. Lebiedowicz, W. Schäfer and A. Szczurek, Phys. Rev. D **83** (2011) 114004.
10. W. Schäfer and A. Szczurek, Phys. Rev. D **76** (2007) 094014.
11. T. Aaltonen *et al.* [CDF Collaboration], Phys. Rev. Lett. **102** (2009) 242001 .
12. K. Kutak and A. M. Staśto, Eur. Phys. J. C **41** (2005) 343 .
13. G. Baur, K. Hencken, D. Trautmann, S. Sadovsky and Y. Kharlov, Phys. Rept. **364** (2002) 359.
14. A. Cisek, W. Schäfer and A. Szczurek, Phys. Rev. C **86** (2012) 014905.
15. N. N. Nikolaev, W. Schäfer and G. Schwiete, Phys. Rev. D **63** (2001) 014020.
16. N. N. Nikolaev, W. Schäfer, B. G. Zakharov and V. R. Zoller, JETP Lett. **84** (2007) 537.